The mechanics of subglacial sediment: an example of new "transitional" behaviour

Fatin Altuhafi, Béatrice A. Baudet, and Peter Sammonds

Abstract: A series of isotropic compression tests and drained and undrained triaxial compression tests have been performed on glacial sediment from Iceland. Langjökull sediment, which is well graded, is thought to have reached a critical grading during deposition and transportation. Multiple parallel normal compression lines (NCLs) were found, but a unique critical state line (CSL) could be identified. This is unlike other so-called "transitional" soils, whose grading varies between reasonably well graded to gap graded, which tend to have distinct NCLs and critical state lines depending on the specimen density. It is thought that in the case of the Langjökull sediment studied, its particular strain history that involved incessant shearing during deposition accounts for the difference in behaviour. This provides the interesting case of a soil that has been crushed to a critical grading in situ, which depends on the mineralogy of the grains, which was then sampled and tested. Despite the unique grading, samples with a range of different void ratios can be prepared and the combination of grading and density seems to set a fabric that cannot be changed by compression, resulting in multiple parallel NCLs. At the critical state, however, the fabric has been destroyed and the CSL is unique.

Key words: glacial soil, particle-size distribution, laboratory tests, critical-state soil mechanics.

Résumé : Une série d'essais en compression isotrope et d'essais en compression triaxiale drainés et non drainés a été effectuée sur des sédiments glaciaires provenant de l'Islande. Les sédiments de Langjökull, qui ont une granulométrie continue, ont possiblement atteint une granulométrie critique durant la déposition et le transport. Plusieurs lignes de compression normales (LCN) parallèles ont été trouvées, mais une seule ligne d'état critique (LEC) a pu être identifiée. Ceci diffère d'autres sols appelés « de transition », qui eux présentent une granulométrie variant entre continue et discontinue, ceux-ci ayant des lignes de compression normales et d'état critique dépendamment de la densité de l'échantillon. Il est postulé que dans le cas des sédiments étudiés de Langjokull, leur historique de contrainte particulière de cisaillement continu durant la déposition a contribué à leur différence de comportement. Ceci fourni un cas intéressant de sol ayant été broyé in situ à une granulométrie critique, qui elle dépend de la minéralogie des grains. Ce sol a été échantillonné et testé. Malgré la granulométrie unique, des échantillons ayant des indices des vides différents peuvent être préparés. La combinaison de la granulométrie et de la densité semble fixer une matrice qui ne peut pas être modifiée par la compression, ce qui produit plusieurs LCN parallèles. Cependant, à l'état critique, la matrice est détruite et la LEC est unique.

Mots-clés : sol glaciaire, distribution granulométrique, essais en laboratoire, mécanique des sols à l'état critique.

[Traduit par la Rédaction]

Introduction

Glacier beds have traditionally been considered to be rigid, but an increasing number of modern glaciers have been found to rest on deformable beds; for example, Breiðamérkurjökull in southeastern Iceland (Boulton and Hindmarsh 1987), Tapridge Glacier in Yukon Territory, Canada (Blake et al. 1992), Storglaciären in Sweden (Iverson et al. 1995), and Bakaninbreen in Svalbard (Porter et al. 1997). Accelerating summer melts have caused ice caps to lose ice volumes and reveal sediments that show a clear stamp of deformation, with shearing caused by glacier movement usually resulting in the remoulding of the upper part of the sediment (e.g., Breiðamérkurjökull, Boulton and Hindmarsh 1987). The implications of deformation of the glacier bed are potentially far reaching in terms of understanding glacier dynamics and the stability of ice sheets. Studies on the behaviour of glacial sediment are, however, limited, with previous research generally focusing on the ultimate strength of the sediments (Kamb 1991; Iverson et al. 1998; Iverson et al. 1999; Tulaczyk 1999; Tulaczyk et al. 2000) or on the sensitivity of the sediments to the rate of shearing (Boulton and Jones 1979; Boulton and Hindmarsh 1987; Blake et al. 1992; Dobbie 1992; Iverson et al. 1998; Truffer et al. 2000;

Received 10 February 2009. Accepted 2 November 2009. Published on the NRC Research Press Web site at cgj.nrc.ca on 23 June 2010.

F. Altuhafi. Department of Civil and Environmental Engineeering, Imperial College London, South Kensington campus, London, SW7 2AZ, UK.
B.A. Baudet.[1,2] Department of Civil, Environmental and Geomatic Engineeering, University College London, Gower Street, London, WC1E 6BT, UK.
P. Sammonds. Department of Earth Sciences, University College London, Gower Street, London, WC1E 6BT, UK.

[1]Corresponding author (e-mail: b.baudet@ucl.ac.uk).
[2]Present address: Department of Civil Engineering, University of Hong Kong, Pokfulam Road, Hong Kong.

Fig. 1. Particle-size distribution of Langjökull sediment.

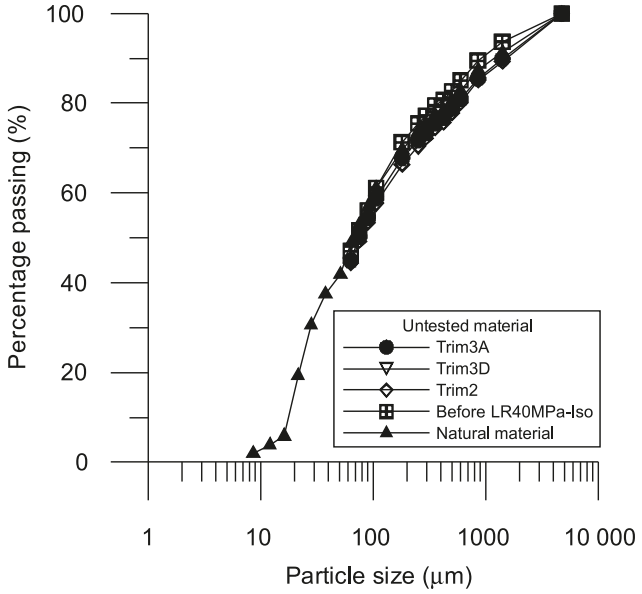

Tulaczyk et al. 2000; Tulaczyk 2006; Altuhafi et al. 2009). This paper presents data from laboratory tests that were performed on glacial sediment from Iceland — Langjökull till — using techniques and theories of geotechnical engineering, in particular critical-state soil mechanics (Roscoe et al. 1958). As well as providing an insight into the mechanical behaviour of an unusual sediment, this paper aims to contribute to current research on glacier movement on deformable beds. The shearing rate–dependency of the till, which has been presented in Altuhafi et al. (2009), is not included here.

Material and sample preparation

Langjökull sediment was retrieved from a proglacial site at the retreated margin of Vestari-Hagafellsjökull in the Langjökull ice cap (Iceland), during a sampling expedition that was part of the Natural Environment Research Council (NERC) ARCICE joint project between University College London (UCL), the University of Southampton, and the University of Bristol. Langjökull is Iceland's second largest ice cap, with an area in 1973 of 953 km^2 and a maximum elevation of 1450 m above sea level. The ice cap provides an ideal field area for research because it is relatively accessible, whilst believed to be resting on deformable sediments (Hart 1995; Fuller and Murray 2000). Ten block samples (30 cm × 30 cm × 40 cm) were collected in 1998–1999 from below the topmost 0.4 m of the lodgement till, which is likely to have been remoulded by shear deformation, erosion, and some fluvial disturbance (Boulton 1976). The samples were frozen on site using liquid nitrogen for easier handling and transportation. The freezing technique is considered one of the practical methods to preserve the granular material structure (Mimura 2003), and it is unlikely that the soil mechanical properties have been affected by this freezing, especially for a sediment that has likely been subjected to many cycles of freezing during its history.

Glacial sediments, unlike other common sediments, were deposited beneath glaciers under unique conditions, suffering incessant shearing due to the continuous movement of the glacier and ice flow at the glacier beds. The resulting subglacial erosion and abrasion of rocks provided the main source of debris in the basal layer of the glacier, which eventually became the source material in the case of glacial sediments classified as lodgement till. Lodgement till is formed when the glacial debris are smeared into the deformable bed due to movement of the glacier. In deformable glacier beds, deposition may have occurred as a combination of three different processes: melt-out at the ice–sediment interface, transportation of the sediment within the deforming layer due to glacial flow, and basal shearing (Hart 1995). Langjökull till is an unstratified, unsorted mixture with a wide range of grain sizes, made of detritus carried in the basal debris layer at the bed–glacier interface where the sediment density is high and mutual attrition of particles is severe due to the high frequency of clast to clast contacts (Shilts 1976; Benn 1995; Hooke and Iverson 1995; Hart et al. 2004). It can be described as cohesionless with a high presence of clasts sometimes larger than 100 mm in diameter, occurring in the form of isolated boulders. From the

Fig. 2. Scanning electron microscope images of an undisturbed sample of Langjökull, showing the sediment's particle size range and shape and the voids in the sediment's undisturbed fabric: (*a*) larger scale image showing a highly weathered fine particle in the middle of the undisturbed sample shown in (*b*); (*b*) image showing the range of particle sizes in the sediment.

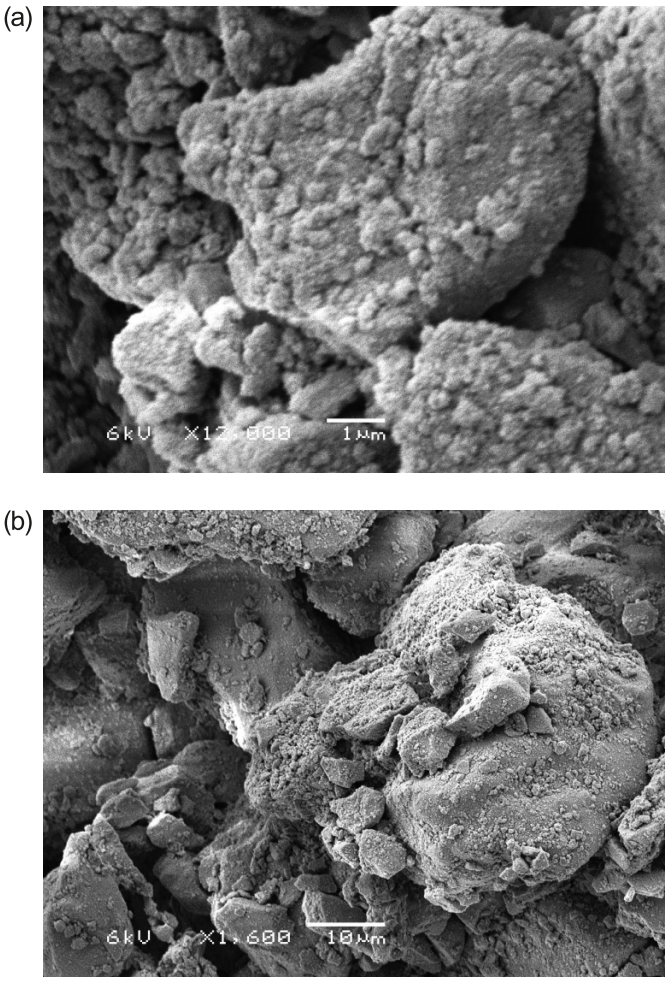

Table 1. Details of isotropic compression tests in the high-pressure triaxial cell (see Fig. 3).

Test	Specimen state	Max. p'_0 (MPa)	$e_{initial}$	e_{final}	e for retrieved specimen*	Remarks
LU-ISO	Undisturbed	37.0	0.57	0.29	0.27	—
LR-ISO	Remoulded	22.0	0.49	0.38	0.39	SEM
LR-30MPa-ISO	Remoulded	30.2	0.42	0.30	0.28	Sieved
LR-40MPa-ISO	Remoulded	40.0	0.52	0.29	0.28	Sieved – SEM

Note: p'_0, mean initial effective pressure; SEM, scanning electron microscope.
*Void ratio calculated from the final water content (of retrieved sample after test), assuming full saturation of the sample.

Table 2. Details of isotropic compression tests in the permeameter (see Fig. 3).

Test	Specimen state	Max. p'_0 (MPa)	$e_{initial}$	e_{final}	e for retrieved specimen*	Remarks
LR250-1	Remoulded	234.0	0.35	0.10	0.066	Sintering
LR250-2	Remoulded	248.3	0.45	0.26	0.17	—
LR250-2A	Remoulded	249.5	0.42	0.23†	0.18†	—
LR250-3	Remoulded	249.0	0.35	0.10	0.10	Sintering

*Void ratio calculated from the final water content (of retrieved sample after test), assuming full saturation of the sample.
†Back pressure system channels experienced some leakage towards the end of test, which resulted in a reduction in the retrieved sample's void ratio.

Fig. 3. Compression curves from isotropic compression tests on Langjökull sediment: undisturbed (LU) and remoulded (LR) specimens.

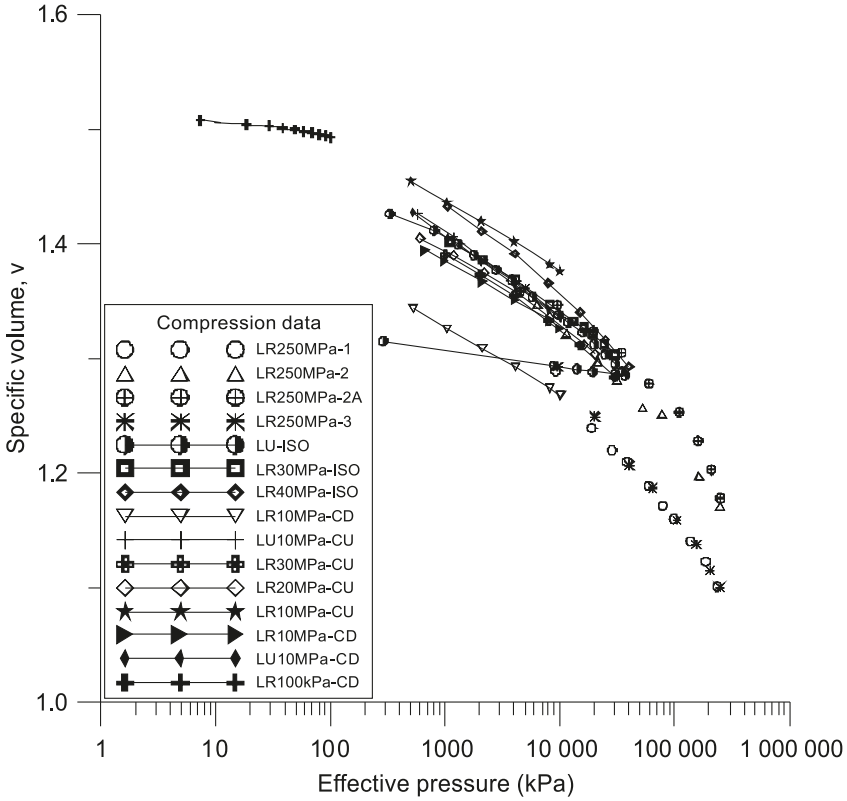

particle-size distribution of the sediment that was tested, shown in Fig. 1, it is seen that the fines count for more than 45% of the sediment. The sediment in the proglacial site was water-saturated, with relatively high void ratios, considering the well-graded nature of the sediment, of around 0.57. The specific gravity was determined to be 3.11. Scanning electron microscopy images of undisturbed samples (Fig. 2) show the subangular, subrounded shape of the sediment particles and the high voids in the sediment's undisturbed fabric. X-ray diffraction test results determined that the sediment is of a typical clean basaltic composition, mainly dominated by feldspar and pyroxenes. The absence of clay minerals in the samples as well as the presence of augite suggest that mechanical weathering rather than chem-

Table 3. Details of triaxial shearing tests on Langjökull sediment at low pressures.

Test	Test description	Specimen state	σ'_r (kPa)	$e_{initial}$	e after consolidation	e_{final}	Shearing rate (mm/h)	Figures
LU1-CU*	CIU	Undisturbed	496	0.58	0.43	0.43	3.0	4, 9, 11, 12, 13
LU2-CU*	CIU†	Undisturbed	215	0.58	0.50	0.50	3.0	4, 9, 11, 12, 13
LR2-CU*	CIU	Remoulded	215	0.48	0.45	0.45	3.0	4, 7*b*, 8*b*,11,12, 13
LR4-CU*	CIU	Remoulded	101	0.52	0.50	0.50	3.0	4, 7*b*, 8*b*, 11, 12, 13
LR3-CU*	CIU	Remoulded	449	0.40	—	—	3.0	4, 7*b*, 8*b*, 11
LR100kPa-CD‡	CID	Remoulded	104	0.51	0.49	0.47	1.0	3, 5*b*, 6*b*, 11,12, 13

Note: σ'_r, effective radial stress at each test; CID, isotropically consolidated drained shearing; CIU, isotropically consolidated undrained shearing.
*Void ratio of retrieved sample was not determined for these tests.
†There was some stress relaxation times during test.
‡Test was conducted in the computer-controlled triaxial cell.

Table 4. Details of triaxial shearing tests in the high pressure triaxial cell.

Test	Sample type	Test type	$e_{initial}$	$e_{start\_shearing}$	e_{final}	Shearing rate (mm/h)	σ'_r (MPa)	e of retrieved specimen	Figures
LU2MPa-CD	Undisturbed‡	CID	0.56*	0.38	0.36	1.0	2.0	0.35	4, 5*a*, 6*a*, 10, 12, 13
LU10MPa-CD	Undisturbed	CID	0.56	0.33	0.29	1.0	10.0	0.27	3, 4, 5*a*, 6*a*, 10, 12, 13
LU10MPa-CU	Undisturbed‡	CIU	0.58	0.33	0.33	3.0	10.2	0.33	3, 4, 7*a*, 8*a*, 10, 12, 13
LR2MPa-CD	Remoulded‡	CID	0.45	0.37	0.35	1.0	2.0	0.33	4, 5*a*, 6*a*, 10, 12, 13
LR2MPa-CD(Dense)	Remoulded‡	CID	0.40	0.36	0.34	1.0	2.1	0.33	4, 5*a*, 6*a*, 10, 12, 13
LR10MPa-CD†	Remoulded‡	CID	0.50	0.33	0.29	1.0	10.0	0.28	3, 4, 5*a*, 6*a*, 10, 12, 13
LR20MPa-CD	Remoulded‡	CID	0.52	0.33	0.27	1.0	20.0	0.27	4, 5*a*, 6*a*, 10, 12, 13
LR30MPa-CD†	Remoulded‡	CID	0.57	0.31	0.27	1.0	30.1	0.25	4, 5*a*, 6*a*, 10, 12, 13
LR10MPa-CU†	Remoulded	CIU	0.47	0.37	0.37	3.0	10.0	0.33	3, 4, 7*a*, 8*a*, 10, 12, 13
LR20MPa-CU	Remoulded‡	CIU	0.49	0.30	0.30	3.0	20.1	0.30	3, 4, 7*a*, 8*a*, 10, 12, 13
LR30MPa-CU	Remoulded	CIU	0.51	0.28	0.28	3.0	30.0	0.28	3, 4, 7*a*, 8*a*, 10, 12, 13

Note: CID, isotropically consolidated drained shearing; CIU, isotropically consolidated undrained shearing.
*Sample experienced some reduction in void ratio when the membrane was placed; initial void ratio due to reduction was 0.50.
†Specimen was sieved before and after test for particle breakage monitoring.
‡Tested using local LVDTs and strain belt.

ical weathering was responsible for the formation of the sediment, concurring with the hypothesis that subglacial deformations played a significant role in the formation of the till (Flint 1971).

The undisturbed samples were trimmed to 38 mm diameter by 76 mm height cylindrical specimens. The trimming was carried out on frozen sediment in a cold room (–20 °C) with the help of a trimming frame that was used to hold the small block of sediment. The trimmed samples were then left to thaw on the pedestal of the apparatus before testing. The remoulded specimens were prepared using the material left from the trimming of the undisturbed samples. Particles with a size larger than 4.75 mm were first removed from the sediment. The remoulded samples were prepared by adding water to the dry sediment to achieve the desirable water content (about 10%). The weight of the sediment was calculated to achieve the desirable void ratio of the sample. The sediment was then statically compacted in three layers in a cylindrical three-part mould made to measure. The three layers were composed of a similar weight of soil and were compacted by applying a static load to achieve a pre-determined thickness. This was done to ensure homogeneity throughout the sample.

This method was also applied to the preparation of the loose specimens because segregation in the well-graded sediment prevented an efficient use of the pluviation method

Fig. 4. Stress ratio versus axial strain for triaxial compression tests on Langjökull sediment.

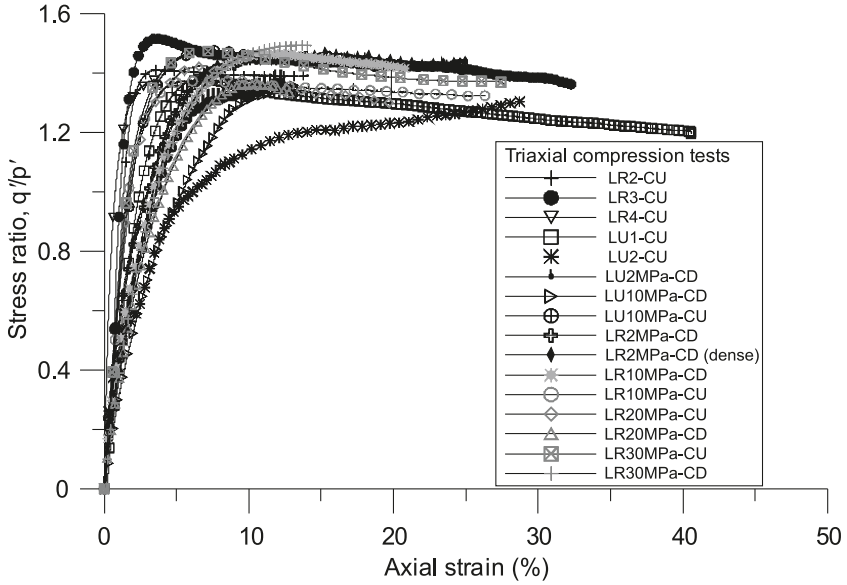

described by Coop and Lee (1993). The loosest specimen prepared in this way had a void ratio of 0.52, which compares well with the void ratio of 0.56–0.58 in the natural material, while the densest specimen had a void ratio of 0.35 to investigate the effect of initial density of the specimen on its behaviour.

Testing apparatus and procedure

Langjökull sediment was deposited under a temperate glacier, and it is usually assumed that such sediment is fully saturated, ice-free, and under high pore-water pressures. In the case of the Langjökull glacier, the pore-water pressures were measured to be of the same order of magnitude as the overburden pressure (Eyre 2003), so that the in situ effective stress is very low, of the order of a few kPa. Because of limited drainage routes, it is usually assumed that deformations underneath glaciers occur in undrained conditions (Boulton and Dobbie 1993; Tulaczyk et al. 2000). Within the programme of tests, it was attempted to replicate these conditions, but testing at very low confining pressures proved difficult. A more comprehensive programme of tests was devised that eventually enabled building a framework for the behaviour of the till. It included tests at low to moderate pressure, up to 1 MPa confining pressure, carried out both in a conventional triaxial apparatus and a hydraulic triaxial apparatus; tests under higher pressures, conducted using a high-pressure triaxial apparatus (10 to 40 MPa); and extremely high isotropic compression pressures were reached using a permeameter, so-named because it was originally designed to determine the permeability of rocks. The permeameter is similar to a high-pressure triaxial cell and can reach a maximum cell pressure of up to 300 MPa. In addition, one-dimensional compression tests were carried out in an oedometer cell modified to enable the application of higher stresses to the sample, up to 20 MPa. A summary of the tests is given in five tables within this paper.

High-pressure triaxial tests

The high-pressure triaxial apparatus used was developed at UCL. The cell, a steel vessel, uses silicone oil to pressurize the specimen up to 60 MPa. It has two interior compartments: the main chamber and a second upper chamber. A backpressure system, which controls the pore-water pressure, is connected to the base of the specimen. Both cell and pore pressures are controlled by 50 mL piston intensifiers that are monitored by transducers logged to a computer. The specimen is sheared by pushing the cell base upward by means of controlled-rate mechanical gears and gear box, with the upper ram fixed to an external frame. The ram, made of specially hardened steel, precision ground, and set in polytetrafluoroethylene (PTFE) seals to minimize friction, is drilled to allow a connection between the main chamber and the upper chamber to balance out the upthrust on the ram from the pressurizing fluid. Shear force and displacement are monitored by an external load cell and externallinear variable displacement transducer (LVDT), respectively. Volume change of the specimen is monitored by the change of water volume in the backpressure system intensifier cylinder, which was calibrated for this purpose. Local LVDTs with an accuracy of 0.0001% were placed on the specimen to measure small deformations. The top and bottom platens receiving the specimen were lubricated to favour a right cylinder deformation of the specimen, so that the change in area of the specimen during testing could be accounted for when calculating the deviatoric stress. The specimens were installed in the triaxial chamber immediately after preparation, and saturation was conducted in stages until a Skempton *B*-value above 0.96 was obtained (Skempton 1954). The cell pressure was then increased to reach to the desired value of effective confining stress. The ram was subsequently pushed downwards until it touched the specimen, using the same strain rate as that used for the shearing. The stabilized readings from the load cell during that stage were used to correct the value of axial force during shearing.

Fig. 5. Deviator stress development during drained triaxial compression test on remoulded specimens: (*a*) high confining pressure; (*b*) low confining pressure (100 kPa).

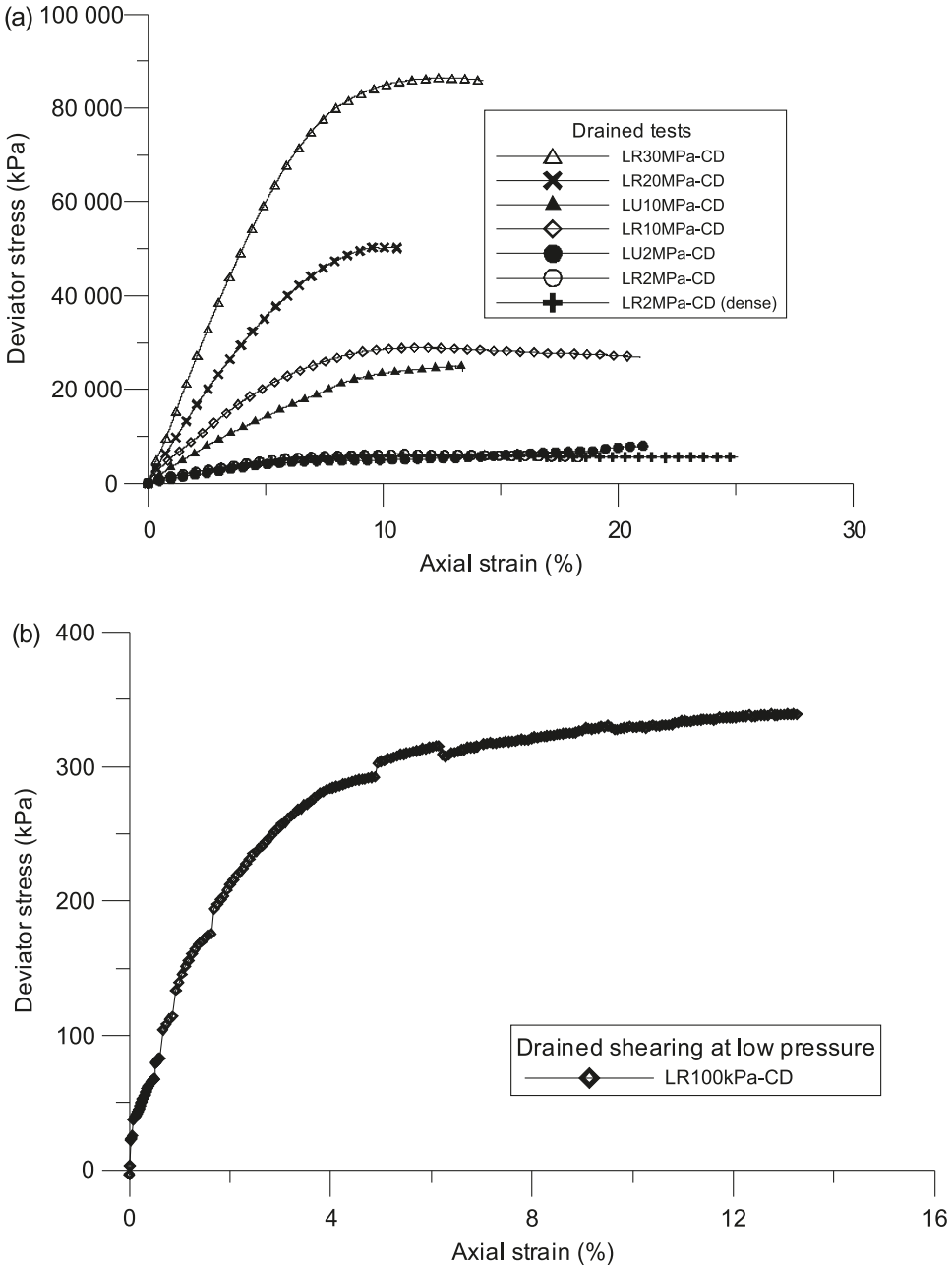

High-pressure permeameter tests

Specimens were constructed in a similar way to those for the triaxial cell, then they were held in a stainless steel frame that was lowered inside the pressure chamber and securely isolated by a breech nut. Backpressure was applied to the top of the specimen using a computer-controlled intensifier. Two transducers were used to monitor the backpressure applied and the pore-water pressure developing inside the specimen. The volume change of the specimen was monitored by the displacement of the piston of the backpressure intensifier, which was calibrated for this purpose. The cell pressure was monitored in two ways: by a pressure gauge and an inline transducer, which logged the data to a computer. Four isotropic compression tests were performed on reconstituted specimens, which reached 250 MPa: two dense specimens (void ratio e = 0.35) and two medium-density specimens (e = 0.41 and 0.43).

Modified oedometer cell

A standard oedometer loading frame along with a special oedometer cell that was modified to enable the application of higher stresses to the specimen by reducing the stress

Fig. 6. Volumetric strain response during drained triaxial compression test on remoulded specimens: (*a*) high confining pressure; (*b*) low confining pressure (100 kPa).

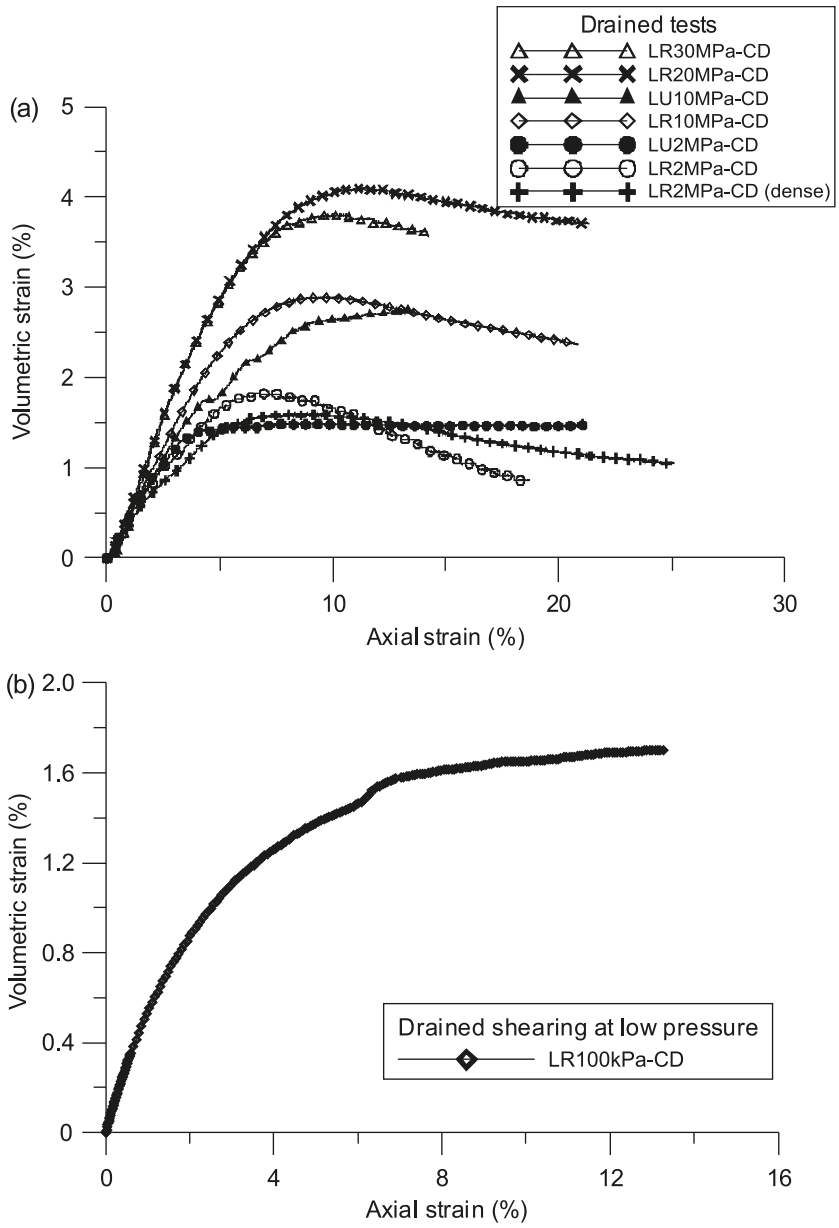

contact area were used. Selection of the modified cell, because of its small size (20 mm diameter by 10 mm height), meant that it was not possible to use intact specimens. The remoulded samples were prepared by pouring a saturated sediment mixture (slurry) into the sample ring to achieve a high void ratio for the tested sample. The initial density of the sample was determined from the dry weight of the sediment poured in the ring and the interior sample ring volume.

Isotropic compression tests and sediment yielding

Five isotropic compression tests were performed in the high-pressure triaxial apparatus: one test was carried out on an undisturbed specimen (LU-ISO) to reach a pressure of 37 MPa, while the remaining tests (LR-ISO, LR-10MPa-ISO, LR-30MPa-ISO, and LR-40MPa-ISO) were carried out on remoulded specimens and reached maximum pressures of 22, 10, 30, and 40 MPa, respectively. To reach very high isotropic pressures, higher than those permitted by the high pressure triaxial cell, the permeameter was used to test four additional specimens. Details of the isotropic compression tests are given in Tables 1 and 2.

The compression curves obtained from these tests are shown in Fig. 3. Consolidation stage data of both drained and undrained compression tests on remoulded and intact samples of the sediment (of which details are presented in Table 3) are also included in the figure to present a more complete picture of the sediment behaviour during compression. Parallel compression curves were obtained, with no

Fig. 7. Deviator stress development during undrained triaxial compression test on remoulded specimens: (*a*) high confining pressure; (*b*) low confining pressure (100 kPa).

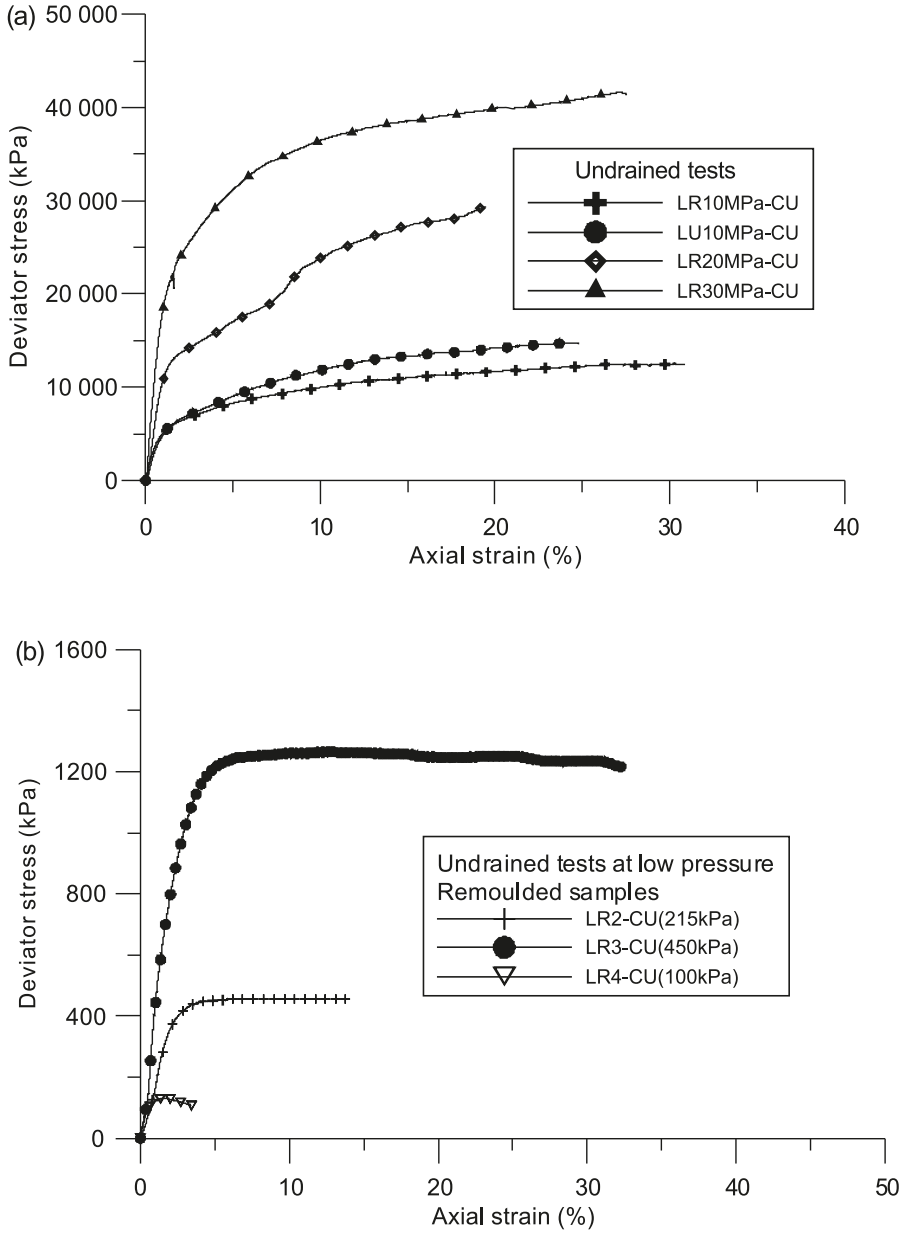

tendency to converge even at the very high pressure of 250 MPa. They seemed to depend on the initial sample's density. Similar trends were found for the undisturbed and remoulded specimens. No clear yielding point could be identified on either curve; however, the higher stiffness obtained from the unloading curves would indicate that deformations in the specimens were elastoplastic.

Similar examples of nonunique normal compression lines (NCLs) have been reported in the literature for remoulded specimens of gap-graded residual soils (Ferreira and Bica 2006), some types of well-graded silts (Nocilla et al. 2006), and some mixed soils (Martins et al. 2001). Langjökull sediment is well graded, with a coefficient of uniformity of $D_{60}/D_{10} = 5.55$, even though this figure does not give a true representation of the wide range of particle sizes present in the sediment, with the fine fraction counting for more than 45%. Previous research, however, has shown that the fractal dimension often provides a better description of granular soils that have suffered particle breakage during their history. Researchers have shown that soils that have undergone particle breakage during compression usually develop a fractal grading (Sammis et al. 1987; McDowell et al. 1996), with typical fractal dimensions of 2.5–2.6. The fractal dimension tends to be higher in materials that are not the result of pure crushing; for example, subglacial sediments that have been subjected to sorting (Hooke and Iverson 1995; McDowell and Bolton 1998; Khatwa et al. 1999). The Langjökull sediment studied here was found to have a fractal dimension

Fig. 8. Excess pore-water pressure development during undrained triaxial compression test on remoulded specimen: (*a*) high confining pressure; (*b*) low confining pressure (100 kPa).

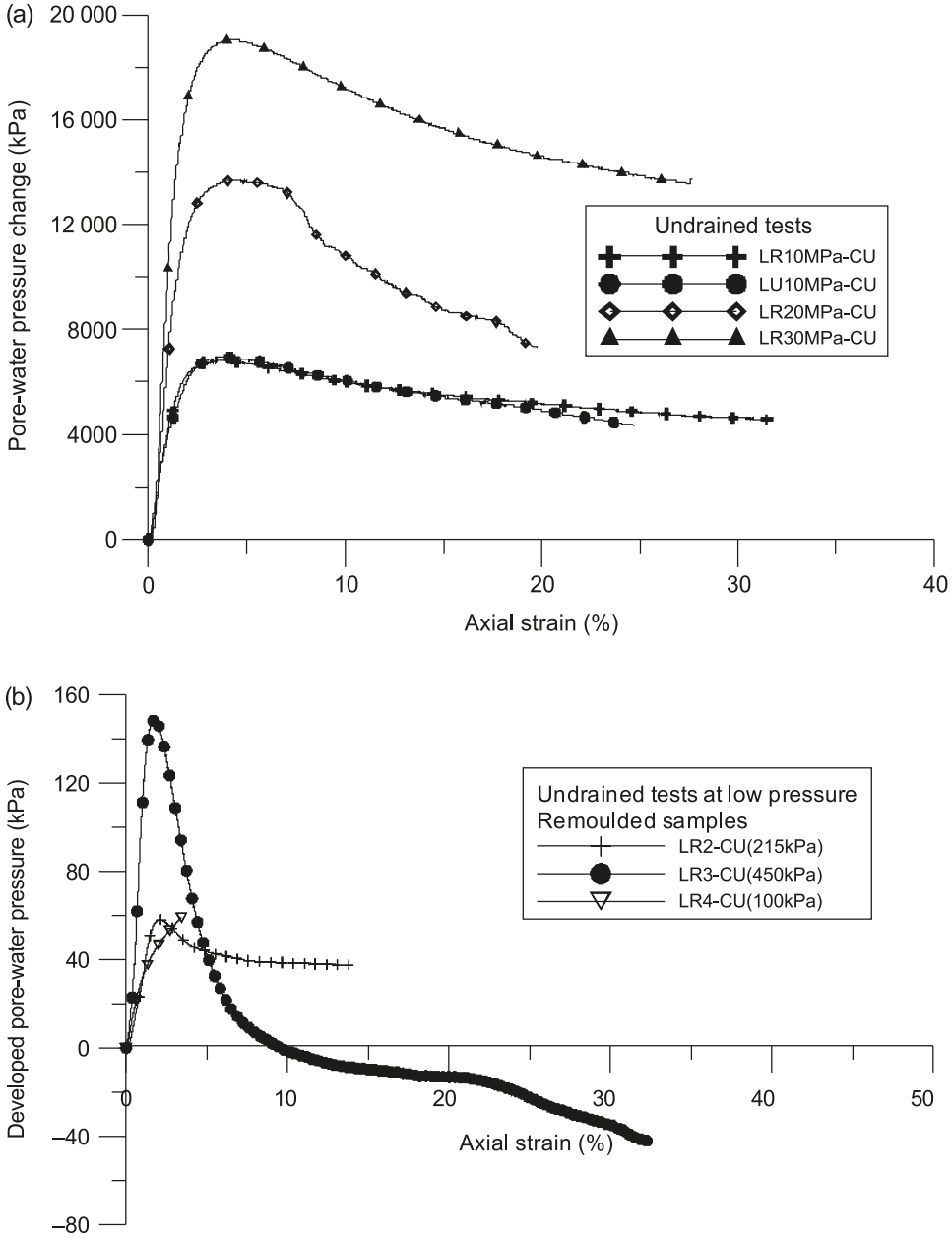

of about 2.9. Studies of particle breakage of Langjökull sediment have further shown that its well-graded particle-size distribution cannot evolve any more when submitted to high stresses and strains, so that the sediment seems to have reached an ultimate grading in the ground (Altuhafi et al. 2006).[3] Yield in granular materials has been associated with particle breakage (Coop and Lee 1993; McDowell and Bolton 1998; Hyodo et al. 2002), and in the case of Langjökull sediment the absence of particle breakage during compression may be associated with the lack of a clear yielding point and perhaps nonconvergence of NCLs. The dependency of the compression curve location on the initial density or void ratio of the specimen, which also seems to be a feature of Langjökull sediment, has been termed "transitional" (Nocilla et al. 2006). This well-defined feature in compression, however, does not extend to the determination of the CSL, where researchers have found it difficult to single-out a unique pattern of behaviour (e.g., Nocilla et al. 2006). This is explored in the following section.

Triaxial compression tests and critical state

Drained and undrained triaxial compression tests were carried out on both reconstituted and undisturbed specimens, using the conventional triaxial cell, the high-pressure triaxial cell, and a fully computer-controlled cell, keeping the cell

[3] Altuhafi, F., Baudet, B.A., and Sammonds, P. On the particle size distribution of glacial sediments. Submitted for publication.

Fig. 9. Response during undrained triaxial compression test on undisturbed specimen: (*a*) deviator stress; (*b*) excess pore-water pressure.

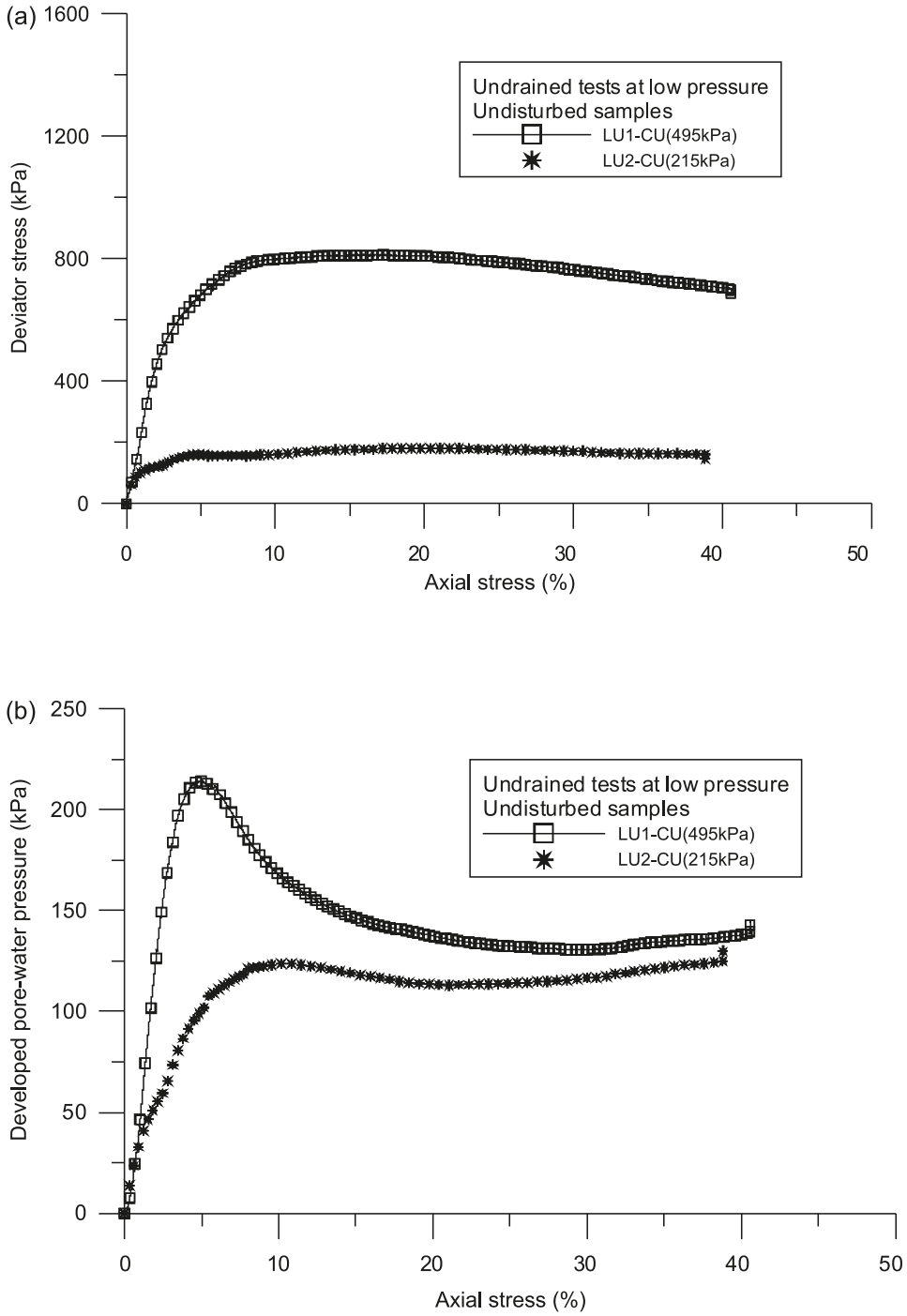

pressure constant during shearing in all tests. The undisturbed specimens were therefore subjected to stresses higher than those they were subjected to in the ground, but because the material is pure basalt, it is not expected to have any structure (Boulton 1976) other than perhaps some fabric which, as a stable form of structure, would not be affected by the isotropic compression prior to shearing. Details of the tests conducted are given in Tables 3 and 4, and results are plotted in the next eight figures. Irrespective of the intact or remoulded nature of the specimens, they all seem to reach a stress ratio of about 1.4 at large strains (Fig. 4). Some specimens strain-harden to failure e.g., LU2-CU, whereas others reach a peak stress ratio around 1.5 followed by strain-softening to failure e.g., LR3-CU, depending on the state of the specimen at the start of shearing.

The stress–strain response during drained shearing of the remoulded specimens is shown in Fig. 5. During the two high-pressure tests at 20 MPa and 30 MPa confining pressure (Fig. 5*a*), the deviator stress could only be logged until 10%–15% axial strain, but the other tests, at 2 MPa and 10 MPa, show good repeatability with mild or no softening until failure. The volumetric response (Fig. 6*a*) indicates a

Fig. 10. Stress paths of tests under high confining pressure, in the deviator stress – mean effective stress plane, showing the CSL.

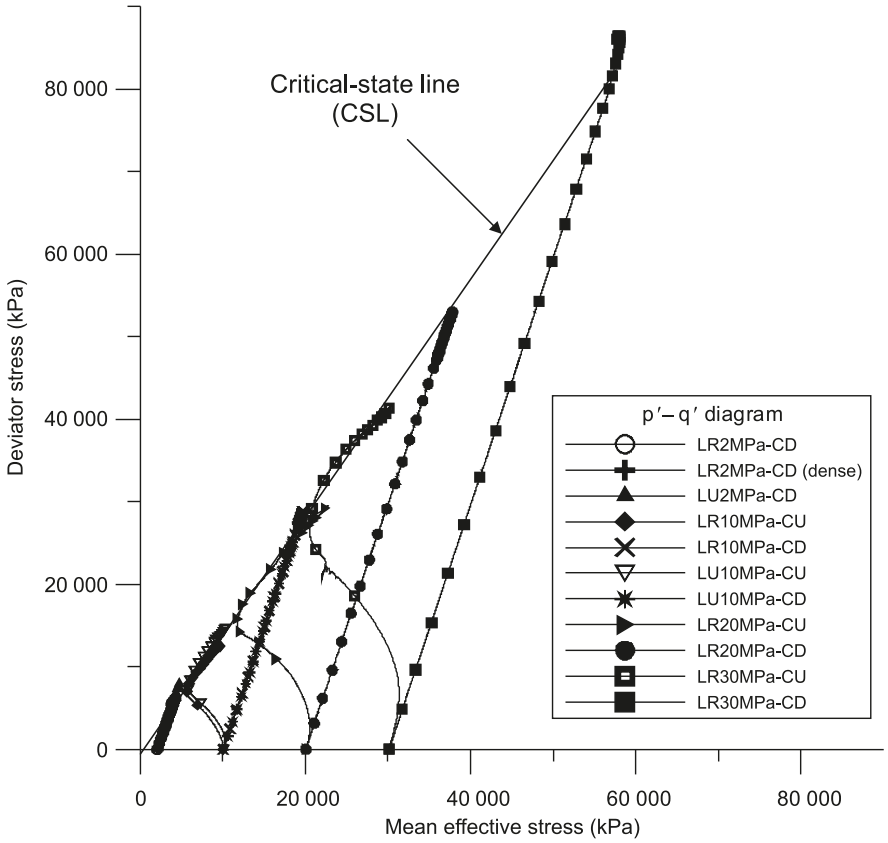

tendency to first contract before dilating, in all these tests except for LU2MPa-CD. The contractive phase is quite long, with the peaks reached at strains between 5% and 10%. Results from the single low-stress test, performed at 100 kPa confining pressure, are shown in Figs. 5*b* and 6*b*. Both stress–strain and volumetric responses are contractive, with the specimen strain-hardening to reach failure at about 10% axial strain.

The stress–strain response and excess pore-water pressure response during undrained shearing of the remoulded specimens is shown in Figs. 7 and 8. During the tests performed at high confining pressure, the specimens uniformly strain-hardened to reach a stable strength at large strains (Fig. 7*a*). The excess pore-water pressure, however, increased to a peak, reached at about 5% axial strain, before decreasing by as much as 30% (Fig. 8*a*). The tests performed at low stresses (Fig. 7*b*) also seem to uniformly strain-harden to a critical state, even though the test at 100 kPa confining pressure was finished prematurely. This is accompanied by a sharp rise in excess pore-water pressure until a peak at about 3% axial strain (Fig. 8*b*), after which the pore pressure reduces, dramatically in one case, perhaps because of the relatively high initial density of the sample (initial $e = 0.40$).

Results from the undrained tests performed on the undisturbed specimens are shown in Fig. 9. These tests were carried out at "low" effective confining pressures of 215 and 495 kPa. As in their remoulded homologues, the specimens strain-hardened to reach a stable critical state (Fig. 9*a*), while the excess pore-water pressure peaked before decreasing to a near stable state (Fig. 9*b*).

The stress paths for all tests and for tests performed at pressures less than 500 kPa are shown in Figs. 10 and 11, respectively. All stress paths seem to indicate a unique CSL in the stress plane, which concurs with the unique stress ratio defined at large strains in Fig. 4. The undrained stress paths obtained from the higher stress tests (Fig. 10) are typical of those obtained on granular materials, with a phase transformation point close to the CSL defining the transition between the contractive and dilative behaviours that were observed in the pore-water pressure responses. Figure 11 details the tests performed at lower confining pressures (100–500 kPa), on both undisturbed and remoulded specimens. Both the intact and remoulded specimens tested at 495 and 450 kPa, respectively, show a similar trend as the higher stress tests, but the contractive phase is less discernible. The two specimens sheared at 215 kPa also seem to follow the same path; however, the intact specimen contracted much more than the remoulded specimen before reaching what seems to be a phase transformation point, but this is not too clear. The remoulded specimen tested at 100 kPa, which was relatively loose (initial $e = 0.52$), developed positive pore-water pressure and veered to the left, as would be predicted by the stress–strain and pore–water pressure responses. From Figs. 4, 10, and 11, a unique CSL can be defined in the stress plane, such that

$$[1] \qquad q' = Mp'$$

where q' is the deviator stress, M (equal to about 1.4) is the gradient of the CSL, and p' is the mean effective pressure. The CSL chosen takes into account the changes in pore-

Fig. 11. Stress paths of tests conducted under low confining pressure, in the deviator stress – mean effective stress plane. The CSL is drawn on the graph.

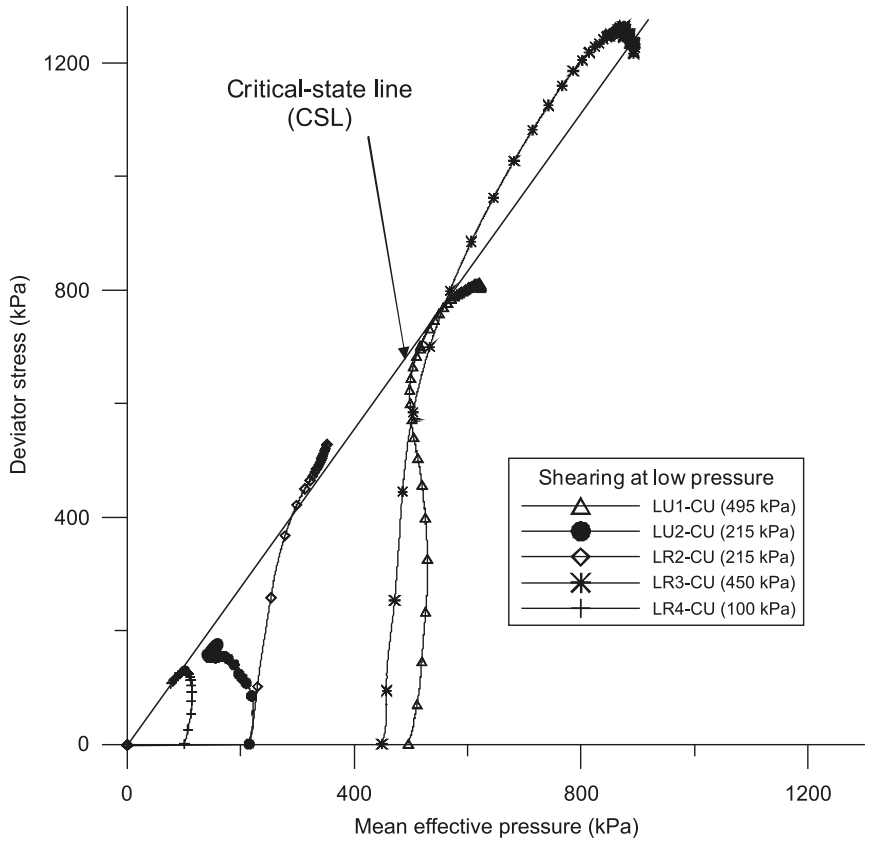

Fig. 12. Stress paths during testing and the CSL in the specific volume – mean effective pressure (logarithmic scale) plane: (*a*) for high-pressure triaxial compression tests; (*b*) all triaxial compression tests in both high and low pressures.

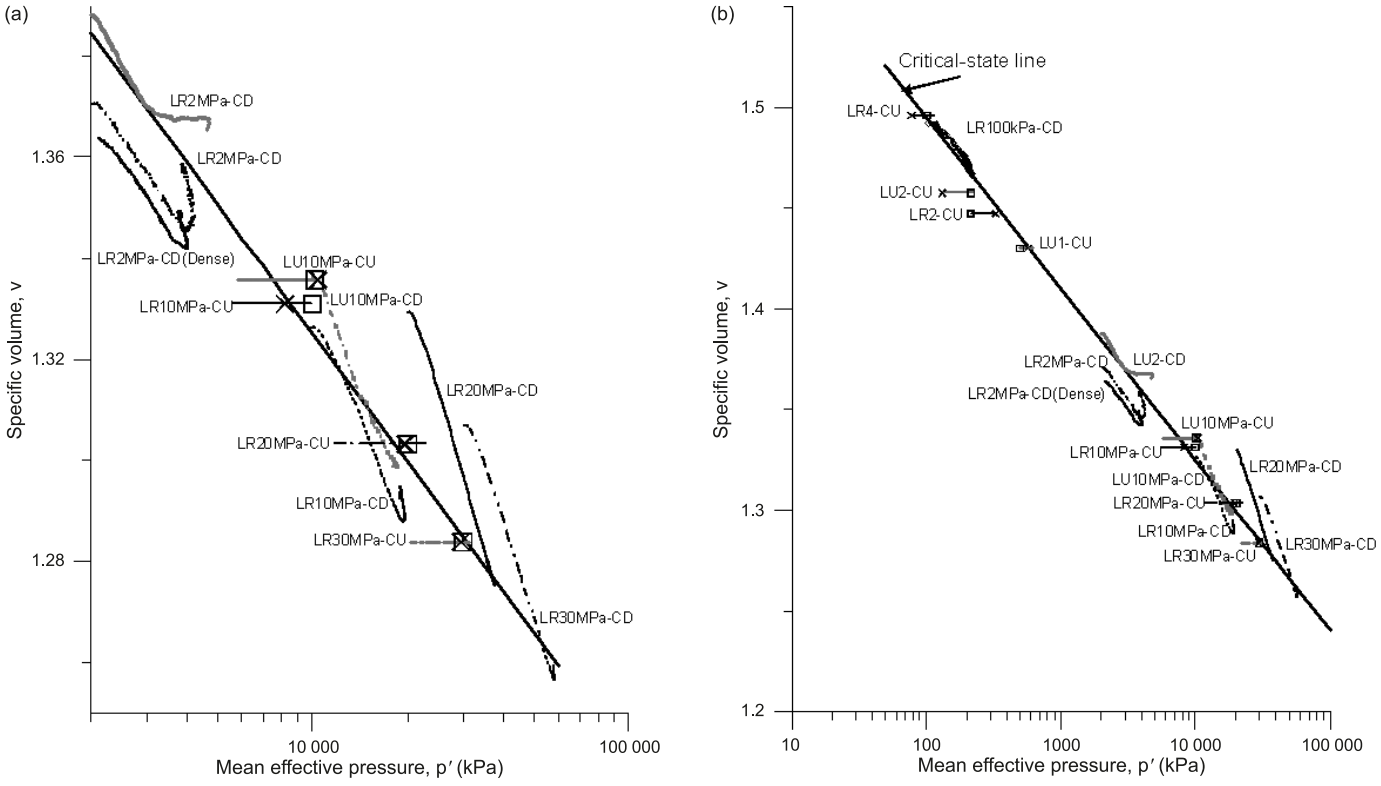

Fig. 13. Normalised stress paths using the equivalent pressure on the CSL, p'_{cs}.

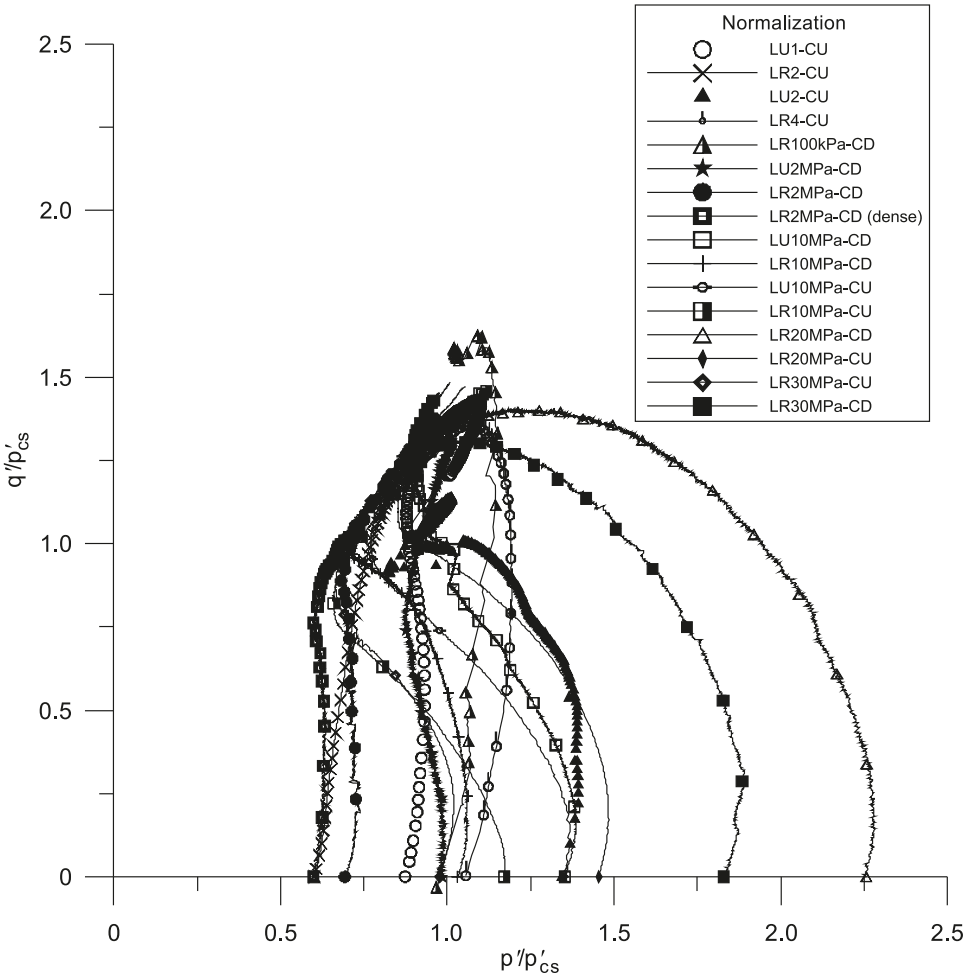

Table 5. Details of one-dimensional compression tests in the modified oedometer cell (see Fig. 14).

Test	$e_{initial}$	Max. p'_0 (MPa)	e_{final}	e of retrieved specimen
LR1-Oedo	0.50	19.8	0.37	0.34
LR2-Oedo	0.61	20.9	0.43	0.43
ART1-Oedo	0.90	14.7	0.59	—
ART2-Oedo	0.97	19.3	0.56	0.50

water pressure still occurring at the end of some tests; however, the value of M should not be taken as accurate because of these uncertainties. Nevertheless, all specimens seem to join a unique CSL in the p'–q' plane, regardless of the undisturbed–remoulded state of the specimen, the initial state of the specimen or the confining pressure at which the specimens were sheared.

Data of the shearing tests performed on the Langjökull sediment are now presented in the volumetric space v–lnp' in Fig. 12, with an inset Fig. 12*a* for detail. The initial and final states of the tests have been marked on the undrained paths. A CSL was drawn, taking into account the small changes in volumetric strain that were still occurring at the end of some tests. The equation for the identified CSL identified is

$$[2] \qquad v = \Gamma - \lambda \ln p'$$

where the gradient $\lambda = 0.037$ and the intercept $\Gamma = 1.664$ at $p' = 1$ kPa. This is a very low value of λ, which should not be taken as an accurate value because of the uncertainty associated with some critical-state points; nevertheless, it compares reasonably well with the gradient of the parallel compression lines in Fig. 3, estimated to be about 0.05.

Having determined the location of the CSL in v–lnp' space, it is now possible to comment on the contractive–dilative response of the sediment to shearing. In uniformly graded granular materials, this response would be attributed to the effect of the void ratio of the specimen at the start of shearing and the initial state of the sediment relative to the CSL (Been and Jefferies 1985; Klotz and Coop 2001). Thus, if the state of the specimen at the start of shearing is located below the CSL, the specimen will dilate upon shearing; while if the initial state is above the CSL, it will exhibit contractive behaviour upon shearing. The concept of state parameter was applied to Langjökull sediment, however because no unique normal compression line (NCL) could be determined, the stress paths were not normalized using the NCL, which usually serves as reference line, but were normalized with the CSL to determine equivalent pressures, p'_{cs}, for given void ratios. A similar

Fig. 14. One-dimensional compression on naturally graded samples and artificially more uniformly graded specimens of Langjökull sediment.

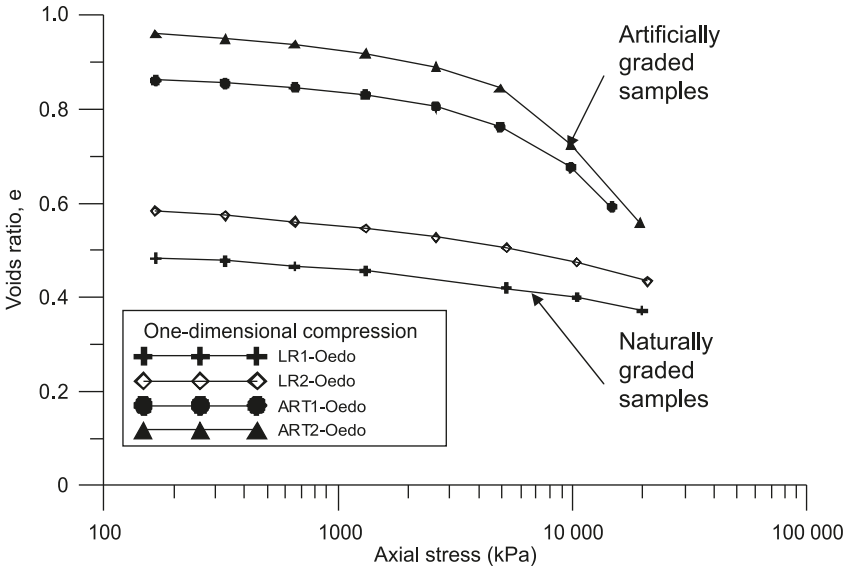

method has been used by others (e.g., Klotz and Coop 2001; Ferreira and Bica 2006). The equivalent pressure on the CSL can be determined using the equation

$$[3] \qquad p'_{cs} = \exp[(\Gamma - v)/\lambda]$$

The normalized stress paths for both drained and undrained tests are shown in Fig. 13. They define a unique locus for critical states at a point of coordinates p'/p'_{cs} = 1.0 and q'/p'_{cs} = 1.4. However, because there is no unique NCL for the sediment, it is not possible to define a boundary surface. For each specimen, there is a unique location defining the start of shearing, which is defined by the state of the specimen itself and its position relative to the CSL. On the dry side of critical, the dense specimens seem to outline a unique Hvorslev surface (Hvorslev 1937).

Discussion

The results from the series of compression and shearing tests on glacial Langjökull specimens have highlighted patterns of behaviour that differ in some parts from that of granular materials. No unique NCL could be determined in the v–lnp' plane, the location of the NCL depending on the initial density of the specimen. In shearing however, a unique CSL could be defined in both the stress and volumetric planes. While the nonuniqueness of the NCL has been found previously by Nocilla et al. (2006) on Italian well-graded silt and by Ferreira and Bica (2006) on gap-graded residual soil, they concurred in not finding a unique CSL for either of these soils. Nocilla et al. (2006) went further by identifying two distinct critical state lines (CSLs) in the q'–p' plane for drained and undrained tests. Previous work by Gens and Potts (1982) had also shown that glacial soil does not follow Rendulic's principle (Rendulic 1936), but because they used the same initial void ratio in all tests it is difficult to state now whether the soil was transitional or not.

In the case of the Langjökull sediment, work presented elsewhere[3] has shown that its grading may be ultimate or critical, so that further breakage in compression or shearing is not possible. It was also found that if the smaller particles (<295 μm) were removed to create a uniformly graded specimen, the coarse-grained sediment created showed marked yielding when compressed one-dimensionally to high stresses (Table 5; Fig. 14). In addition, a single NCL could be identified for the coarse-grained sediment. It thus seems that the well-graded nature of the sediment hinders its capacity to reach a unique NCL, which is usually associated with particle breakage in granular soils (e.g., Coop and Lee 1993). Nocilla et al. (2006) similarly found that, in well-graded Italian silt of low clay content (8% and 3.5%), compression to high stresses does not cause significant particle breakage while no unique NCL can be identified.

Although, the Langjökull sediment may yield in compression, as suggested by the relatively stiff unloading response compared with the loading curve, the initial state of grading and density seems to define the location of the NCL. The agreement between the gradients of the NCL and CSL also seem to indicate that the parallel compression curves are indeed multiple NCLs. The NCL typically reached in other granular soils by crushing particles to high stresses may thus represent a transient behaviour between the original soil and the final soil obtained when all crushing has ceased, as suggested by models including crushing (e.g., Daouadji and Hicher 2006; Muir Wood 2006; Muir Wood 2008). In the case of Langjökull sediment, because it has already reached a critical grading in situ, it seems that its behaviour is uniquely defined by its density, leading to different compression curves for different densities. Density also affects the response during shearing, with different densities showing different behaviours — contractive or dilative — depending on the initial state of the specimens. The CSL, however, is not affected by initial density, as all tested specimens ultimately reached a unique CSL in v–q'–p' space, so that reaching the critical state seems to be reduced to reaching a steady density (or volume) by either dilating or contracting during deformation. This further suggests that

the fabric is completely destroyed during the process of shearing. It also concurs with the assumption that the CSL evolves with changing grading towards a steady state (Muir Wood 2008), but that when there is no further breakage it reaches an ultimate stable position.

Conclusions

Data from a well-graded glacial sediment, which is thought to have reached a critical grading during deposition and transportation, have been presented. Multiple parallel NCLs were found, but a unique CSL could be identified. This is unlike other so-called "transitional" soils, whose grading varies between reasonably well graded to gap graded, which tend to have distinct NCLs and CSLs depending on the specimen density. It is thought that in the case of the studied soil, Langjökull sediment, its particular strain history that involved incessant shearing during deposition accounts for the difference in behaviour. This provides the interesting case of a soil that has been crushed to a critical grading in situ, which depends on the mineralogy of the grains, which was then sampled and tested. Despite the unique grading, samples with different void ratios can be prepared, and the combination of grading and density in each specimen seems to set a fabric that cannot be changed by compression, resulting in multiple parallel NCLs. At the critical state, however, the fabric has been destroyed and the CSL is unique. Further work on similarly well-graded soil is necessary to confirm the behaviour outlined here.

Acknowledgements

The authors would like to thank Dr. Catherine Stafford for the difficult work she carried out in Iceland, resulting in the provision of the specimens that were tested for this study. Prof. Matthew Coop and Dr. Pedro Ferreira must also be acknowledged for their advice on testing and interpreting the soil's data. The tests on the high-pressure devices would also not have been possible without the work and help of Mr. Neil Hughes in the UCL Earth Sciences laboratory.

References

Altuhafi, F., Baudet, B.A., and Sammonds, P. 2006. Particle breakage in glacial sediments. *In* Geomechanics and Geotechnics of Particulate Media, Proceedings of the International Symposium on Geomechanics and Geotechnics of Particulate Media, Ube, Yamaguchi, Japan, 12–14 September 2006. *Edited by* M. Hyodo, H. Murata, and Y. Nakata. Taylor and Francis Group, London. pp. 21–24.

Altuhafi, F.N., Baudet, B.A., and Sammonds, P. 2009. On the time-dependent behaviour of glacial sediments: a geotechnical approach. Quaternary Science Reviews, **28**(7–8): 693–707. doi:10.1016/j.quascirev.2008.07.016.

Been, K., and Jefferies, M. 1985. State parameter for sands. Géotechnique, **35**(2): 99–112. doi:10.1680/geot.1985.35.2.99.

Benn, D.I. 1995. Fabric signature of subglacial till deformation, Breidamerkurjökull, Iceland. Sedimentology, **42**(5): 735–747. doi:10.1111/j.1365-3091.1995.tb00406.x.

Blake, E.W., Clarke, G.K.C., and Gerin, M.C. 1992. Tools for examining subglacial bed deformation. Journal of Glaciology, **38**(130): 388–396.

Boulton, G.S. 1976. The development of geotechnical properties in glacial till. *In* Glacial till. Special Publication No. 12. *Edited by* R.F. Lagget. The Royal Society of Canada, Ottawa, Ont. pp. 292–303.

Boulton, G.S., and Dobbie, K.E. 1993. Consolidation of sediments by glaciers; relations between sediment geotechnics, soft-bed glacier dynamics and subglacial ground water flow. Journal of Glaciology, **39**(131): 26–44.

Boulton, G.S., and Hindmarsh, R.C.A. 1987. Sediment deformation beneath glaciers: rheology and geological consequences. Journal of Geophysical Research, **92**(B9): 9059–9082. doi:10.1029/JB092iB09p09059.

Boulton, G.S., and Jones, A.S. 1979. Stability of temperate ice caps and ice sheets resting on beds of deformable sediment. Journal of Glaciology, **24**(90): 29–43.

Coop, M.R., and Lee, I.K. 1993. The behaviour of granular soils at elevated stresses. *In* Predictive soil Mechanics, Proceedings of the Wroth Memorial symposium, Oxford, UK, 27–29 July 1992. *Edited by* B.G.S. Parry and R.H.G. Parry. Thomas Telford, London. pp. 186–198.

Daouadji, A., and Hicher, P.Y. 2006. Modeling influence of grain breakage. *In* Geomechanics and Geotechnics of Particulate Media, Proceedings of the International Symposium on Geomechanics and Geotechnics of Particulate Media, Ube, Yamaguchi, Japan, 12–14 Septmber 2006. *Edited by* M. Hyodo, H. Murata, and Y. Nakata. Taylor and Francis Group, London. pp. 319–325.

Dobbie, K.E. 1992. Till geotechnics and ice sheets dynamics. Ph.D. thesis, University of Edinburgh, Edinburgh, UK.

Eyre, N. 2003. The role of subglacial processes in glacial dynamics. Ph.D. thesis, University of Bristol, Bristol, UK.

Ferreira, P.M., and Bica, A.V.D. 2006. Problems in identifying the effects of structure and critical state in a soil with transitional behaviour. Géotechnique, **56**(7): 445–454. doi:10.1680/geot.56.7.445.

Flint, R.F. 1971. Glacial and quaternary geology. John Wiley and Sons, Inc., New York.

Fuller, S., and Murray, T. 2000. Evidence against pervasive bed deformation during the surge of an Icelandic glacier. *In* Deformation of glacial materials. Geological Society Special Publication No. 176. *Edited by* A.J. Maltman, B. Hubbard, and M.J. Hambrey. The Geological Society, London. pp. 203–216.

Gens, A., and Potts, D.M. 1982. A theoretical model for describing the behaviour of soils not obeying Rendulic's principle. *In* Proceedings of the International Symposium on Numerical Models in Geomechanics, Zurich, Switzerland, 13–17 September 1982. *Edited by* R. Dungar, G.N Pandes, and J.A. Studer. A.A. Balkema, Rotterdam, the Netherlands. pp. 24–32.

Hart, J.K. 1995. Subglacial erosion, deposition and deformation associated with deformable beds. Progress in Physical Geography, **19**(2): 173–191. doi:10.1177/030913339501900202.

Hart, J.K., Khatwa, A., and Sammonds, P. 2004. The effect of grain texture on the occurrence of microstructural properties in subglacial till. Quaternary Science Reviews, **23**(23-24): 2501–2512. doi:10.1016/j.quascirev.2004.06.006.

Hooke, R.L., and Iverson, N.R. 1995. Grain size distribution in deforming subglacial tills: role of grain fracture. Geology, **23**(1): 57–60. doi:10.1130/0091-7613(1995)023<0057:GSDIDS>2.3.CO;2.

Hvorslev, M. J. 1937. Iber die Festigkeitseigenschaften Gestörter Bindiger Böden, Copenhagen, Denmark. [In Danish.]

Hyodo, M., Hyde, A.F.L., Aramaki, N., and Nakata, Y. 2002. Undrained monotonic and cyclic shear behaviour of sand under low and high confining stresses. Soils and Foundations, **42**(3): 63–76.

Iverson, N.R., Hanson, B., Hooke, R.L., and Jansson, P. 1995. Flow mechanisms of glaciers on soft beds. Science, **267**(5194): 80–81. doi:10.1126/science.267.5194.80. PMID:17840062.

Iverson, N.R., Hooyer, T.S., and Baker, R.W. 1998. Ring shear studies of till deformation; Coulomb plastic behaviour and distributed strain in glacier beds. Journal of Glaciology, **44**(148): 634–641.

Iverson, N.R., Baker, R.W., Hooke, R., Le, B., Hanson, B., and Jansson, P. 1999. Coupling between a glacier and a soft bed: A relation between effective pressure and local shear stress determined from till elasticity. Journal of Glaciology, **45**(149): 31–40.

Kamb, B. 1991. Rheological nonlinearity and flow instability in the deforming bed mechanism of ice stream motion. Journal of Geophysical Research, **96**(B10): 16585–16595. doi:10.1029/91JB00946.

Khatwa, A., Hart, J.K., and Payne, A.J. 1999. Grain textural analysis across a range of glacial facies. Annals of Glaciology, **28**(1): 111–117. doi:10.3189/172756499781821913.

Klotz, E.U., and Coop, M.R. 2001. An investigation of the effect of soil state on the capacity of driven piles in sands. Géotechnique, **51**(9): 733–751. doi:10.1680/geot.2001.51.9.733.

Martins, F.B., Bressani, L.A., Coop, M.R., and Bica, A.V.D. 2001. Some aspects of the compressibility behaviour of a clayey sand. Canadian Geotechnical Journal, **38**(6): 1177–1186. doi:10.1139/cgj-38-6-1177.

McDowell, G., and Bolton, M. 1998. On the micromechanics of crushable aggregates. Géotechnique, **48**(5): 667–679. doi:10.1680/geot.1998.48.5.667.

McDowell, G.R., Bolton, M.D., and Robertson, D. 1996. The fractal crushing of granular materials. Journal of the Mechanics and Physics of Solids, **44**(12): 2079–2101. doi:10.1016/S0022-5096(96)00058-0.

Mimura, M. 2003. Characterisitics of some Japanese natural sands — data from undisturbed frozen samples. *In* Characterisation and engineering properties of natural soils. *Edited by* T.S. Tan, K.K. Phoon, D.W. Hight, and S. Leroueil. Swets and Zetlinger, Lisse, the Netherlands. pp. 1149–1168.

Muir Wood, D. 2006. Geomaterials with changing grading: A route towards modelling. *In* Geomechanics and Geotechnics of Particulate Media, Proceedings of the International Symposium on Geomechanics and Geotechnics of Particulate Media, Ube, Yamaguchi, Japan, 12–14 September 2006. *Edited by* M. Hyodo, H. Murata, and Y. Nakata. Taylor and Francis Group, London. pp. 313–325.

Muir Wood, D. 2008. Critical states and soil modelling. *In* Proceedings of the Fourth International Symposium on Deformation Characteristics of Geomaterials, Atlanta, Ga., 22–24 September 2008. *Edited by* S. Burns, P. Mayne, and C. Santamarina. IOS press, Amsterdam, the Netherlands. pp. 51–72.

Nocilla, A., Coop, M.R., and Colleselli, F. 2006. The mechanics of an Italian silt: an example of "transitional" behaviour. Géotechnique, **56**(4): 261–271. doi:10.1680/geot.2006.56.4.261.

Porter, S.C., Murray, T., and Dowdeswell, J.A. 1997. Sediment deformation and basal dynamics beneath a glacier surge from: Bakaninbreen, Svalbard. Annals of Glaciology, **24**: 21–26.

Rendulic, L. 1936. Relation between void ratio and effective principal stresses for remoulded, silty clay: Discussion. *In* Proceedings of the 1st International Conference on Soil Mechanics and Foundation Engineering, Boston, Mass., 22–26 June 1936. Delft Geotechnics, Delft, the Netherlands. pp. 48–51.

Roscoe, K.H., Schofield, A.N., and Wroth, C.P. 1958. On the yielding of soils. Géotechnique, **8**(1): 22–53. doi:10.1680/geot.1958.8.1.22.

Sammis, C., King, G., and Biegel, R. 1987. The kinematics of gouge deformation. Pure and Applied Geophysics, **125**(5): 777–812. doi:10.1007/BF00878033.

Shilts, W.W. 1976. Glacial till and mineral exploration. *In* Glacial till: an interdisciplinary study. *Edited by* F. Robert Legget. Special Publication No. 12. Royal Society of Canada, Ottawa, Ont. pp. 205–224.

Skempton, A.W. 1954. Pore-pressure coefficients A and B. Géotechnique, **4**(4): 143–147. doi:10.1680/geot.1954.4.4.143.

Truffer, M., Harrison, W.D., and Echelmeyer, K.A. 2000. Glacier motion dominated by processes deep in underlying till. Journal of Glaciology, **46**(153): 213–221. doi:10.3189/172756500781832909.

Tulaczyk, S.M. 1999. Basal mechanics and geologic record of ice streaming, West Antarctica. Ph.D. thesis, California Institute of Technology, Pasadena, Calif.

Tulaczyk, S.M. 2006. Fast glacier flow and ice streaming. *In* Glacier Science and Environment Change. *Edited by* P.G. Knight. Blackwell Science Ltd., Oxford, UK. pp. 353–359.

Tulaczyk, S., Kamb, W.B., and Engelhardt, H.F. 2000. Basal mechanics of Ice Stream B, West Antarctica. Journal of Geophysical Research, **105**(B1): 463–481. doi:10.1029/1999JB900329.